nature

https://doi.org/10.1038/s41586-020-2355-0

Accelerated Article Preview

Viral and host factors related to the clinical outcome of COVID-19

Received: 14 March 2020

Accepted: 13 May 2020

Accelerated Article Preview Published online 20 May 2020

Cite this article as: Zhang, X. et al. Viral and host factors related to the clinic outcome of COVID-19. *Nature* https://doi.org/10.1038/s41586-020-2355-0 (2020).

Xiaonan Zhang, Yun Tan, Yun Ling, Gang Lu, Feng Liu, Zhigang Yi, Xiaofang Jia, Min Wu, Bisheng Shi, Shuibao Xu, Jun Chen, Wei Wang, Bing Chen, Lu Jiang, Shuting Yu, Jing Lu, Jinzeng Wang, Mingzhu Xu, Zhenghong Yuan, Qin Zhang, Xinxin Zhang, Guoping Zhao, Shengyue Wang, Saijuan Chen & Hongzhou Lu

Article

Viral and host factors related to the clinical outcome of COVID-19

https://doi.org/10.1038/s41586-020-2355-0

Received: 14 March 2020

Accepted: 13 May 2020

Published online: 20 May 2020

Xiaonan Zhang[1,7], Yun Tan[2,7], Yun Ling[1,7], Gang Lu[2,7], Feng Liu[2,7], Zhigang Yi[1,4,7], Xiaofang Jia[1], Min Wu[1], Bisheng Shi[1], Shuibao Xu[1], Jun Chen[1], Wei Wang[1], Bing Chen[2], Lu Jiang[2], Shuting Yu[2], Jing Lu[2], Jinzeng Wang[2], Mingzhu Xu[1], Zhenghong Yuan[4], Qin Zhang[5], Xinxin Zhang[3], Guoping Zhao[6], Shengyue Wang[2]✉, Saijuan Chen[2]✉ & Hongzhou Lu[1]✉

In December 2019, the Coronavirus disease 2019 (COVID-19), caused by a novel coronavirus SARS-CoV-2, emerged in Wuhan, Hubei province, China[1] and soon spread across the world. In this ongoing pandemic, public health concerns and the urgent need for effective therapeutic measures require a deep understanding of its epidemiology, transmissibility and pathogenesis. Here we analyzed the clinical, molecular and immunological data from 326 confirmed cases of COVID-19 in Shanghai. Genomic sequences of SARS-CoV-2 assembled from 112 quality samples together with sequences in the Global Initiative on Sharing All Influenza Data (GISAID) showed a stable evolution and suggested two major lineages with differential exposure history during the early phase of the outbreak in Wuhan. Nevertheless, they exhibited similar virulence and clinical outcomes. Lymphocytopenia, especially the reduced $CD4^+$ and $CD8^+$ T cell counts upon admission, was predictive of disease progression. High levels of IL-6 and IL-8 during treatment were observed in patients with severe or critical disease and correlated with decreased lymphocyte count. The determinants of disease severity seemed to stem mostly from host factors such as age, lymphocytopenia, and its associated cytokine storm, whereas viral genetic variation did not significantly affect the outcomes.

The COVID-19 outbreak emerged in Wuhan with a strong link to contacts with a seafood market (Huanan Seafood Wholesale Market, HSWM). The causal agent, severe acute respiratory syndrome coronavirus 2 (SARS-CoV-2)[1,2], is closely related to a bat coronavirus (RaTG13)[2], although its receptor binding domain is more similar to that of pangolin coronaviruses[3]. Currently, several questions remain regarding its origin, evolution, and interaction with host. First, although HSWM is widely thought to be the original outbreak site of SARS-CoV-2, a significant number of the initial cases did not have contact with this market[4]. This casts doubt on the singular event of zoonotic spillover to human in the initial outbreak. Second, whether SARS-CoV-2 virulence has altered, due to genomic sequence evolution during the spread of the disease, remains to be answered with additional data. Third, although SARS-CoV-2 infection can cause life-threatening respiratory disease, most cases manifested mild pneumonia[5]. The factors associated with disease outcome are yet to be fully characterized. Here we systematically analyzed key immunological parameters spanning the course of infection, obtained viral genomes directly from clinical samples, and delineated factors associated with prognosis and epidemiological features.

Overview of the enrollment

The basic clinical and epidemiological information of the cohort (326 patients in Shanghai between Jan 20th and Feb 25th) was shown in Extended Data Table 1. Four categories of infected cases were defined. Five individuals were *asymptomatic* as having no obvious fever, respiratory symptoms or radiological manifestations. A majority of the patients (293) had *mild* disease with fever and radiological manifestations of pneumonia. There were 12 patients with symptoms of dyspnea and signs of expanding ground-glass opacity in the lung within 24-48 hours hence defined as *severe* cases. Another 16 patients deteriorated into acute respiratory distress syndrome (ARDS) and required mechanical ventilation or extracorporeal membrane oxygenation (ECMO) and thus were categorized as *critical* (Extended Data Table 1). As of April 1st, 315 (96.63%) patients had been discharged; 6 (1.84%) had deceased.

Nucleotide variation in viral genomes

Sequencing data from 112 samples (sputum, oropharyngeal swab) passed quality control and were used for nucleotide variation

[1]Shanghai Public Health Clinical Center, Fudan University, Shanghai, China. [2]National Research Center for Translational Medicine, Shanghai Institute of Hematology, State Key Laboratory of Medical Genomics, Ruijin Hospital Affiliated to Shanghai Jiao Tong University (SJTU) School of Medicine, Shanghai, China. [3]Research Laboratory of Clinical Virology, Ruijin Hospital Affiliated to Shanghai Jiao Tong University (SJTU) School of Medicine, Shanghai, China. [4]Key Laboratory of Medical Molecular Virology, Shanghai Medical College, Fudan University, Shanghai, China. [5]Tong Ren Hospital, Shanghai Jiao Tong University School of Medicine, Shanghai, China. [6]Institute of Plant Physiology and Ecology, Shanghai Institutes for Biological Sciences, Chinese Academy of Sciences, Beijing, China. [7]These authors contributed equally: Xiaonan Zhang, Yun Tan, Yun Ling, Gang Lu, Feng Liu, Zhigang Yi. ✉e-mail: wsy12115@rjh.com.cn; sjchen@stn.sh.cn; luhongzhou@shphc.org.cn

calling (Extended Data Fig. 1). Compared to the first released genome (Wuhan-Hu-1), a total of 66 synonymous and 103 nonsynonymous variants were identified in nine protein coding regions (Extended Data Fig. 2a-b). Substitution rates of ORF1ab, S, ORF3a, E, M and ORF7a were similar (~3.5×10^{-4} per site per year), while variation rates of the ORF8 (9.51×10^{-4} per site per year) and N (1.05×10^{-3} per site per year) were higher (Extended Data Fig. 2a-b). The recurrence of variations in the viral genome is similar between Shanghai samples and the GISAID dataset (Extended Data Fig. 2c).

Genomic phylogeny analysis

We next used the viral genomes of 94 cases (>90% complete) together with 221 sequences of SARS-CoV-2 in the GISAID database for phylogeny analysis. Two major clades were identified (Fig. 1, Extended Data Fig. 3a-b), both of which included cases diagnosed in early December 2019[1,2]. Clade I included several subclades, such as those characterized by ORF3a: p.251G>V (subclade V), or S: p.614D>G (subclade G). Clades II is distinguished from Clade I by two linked variations ORF8: p.84L>S (28144T>C) and ORF1ab: p.2839S (8782C>T) (Fig. 1, Extended Data Fig. 3a). The sequences of the Shanghai cohort were found throughout the two major clades and their subclades, suggesting multiple origins of transmission into Shanghai. No significant expansion of clades/subclades in Shanghai was observed.

Additionally, six cases with clear contact history to HSWM[1,2], the suspected initial outbreak site, were all clustered into clade I, while three cases diagnosed at the same period without contact history to HSWM[6,7] were all clustered into clade II (Fig. 1). The sequences around nt8,782 and nt28,144 of SARS-CoV-2 were analyzed in HSWM/non-HSWM-related samples and bat coronavirus Bat-SARS-CoV-RaTG13. We noticed that the non-HSWM sequences were identical to Bat-SARS-CoV-RaTG13 at these two sites (Extended Data Fig. 3c).

We compared the clinical manifestations of patients infected with viruses of either clade I or clade II. We found no statistical difference in disease severity (p=0.88), lymphocytes count (p=0.79), CD3 T cell counts (p=0.21), C-reactive protein (p=0.83), or D-dimer (p=0.19), and duration of virus shedding after onset (p=0.79, Extended Data Table 2). Thus, these two clades of viruses exhibited similar pathogenic effects despite their genome sequence variations. Likewise, no significant association was found between disease severity and 13 most frequent variations (synonymous and non-synonymous) (Extended Data Fig. 4).

Host factors associated with disease severity

A notable feature of our cohort was that some infected individuals (5 cases, 1.53%) did not develop obvious symptoms although significant virus shedding could be detected. As shown in Extended Data Fig. 5a, no obvious lesions in the lungs were found in an asymptomatic patient upon admission till five days afterward. In comparison, unilateral and bilateral opacity lesions were observed in a mild (Extended Data Fig. 5b) and a critical case, the latter quickly deteriorated in just two days (Extended Data Fig. 5c).

We further analyzed the immunological and biochemical parameters of the patients (Extended Data Table 3). A prominent feature of COVID-19 was progressive lymphocytopenia, particularly in severe and critical categories (initial test result after admission, $p=6\times10^{-6}$). Detailed analysis of lymphocytes subtypes revealed that $CD3^+$ T cells were most significantly affected ($p<10^{-6}$), with $CD4^+$ and $CD8^+$ T cells sharing similar trends ($CD4^+$ T cell, $p<10^{-6}$; $CD8^+$ T cell, $p=1\times10^{-5}$). Notably, the changes of T lymphocytes were statistically significant not only in critical cases but also in the other three categories (asymptomatic, mild and severe) ($CD3^+$ T cells, p=0.013; $CD8^+$ T cells, p=0.004). By contrast, for $CD19^+$ B cells, although significant decline was found in critical cases ($p=1\times10^{-5}$), no obvious changes were observed among asymptomatic, mild and severe cases (p=0.47). We further examined the longitudinal cell counting data in each group. It was clear that the $CD3^+$ T lymphocytes exhibited graded decline ($p<0.05$ on day 7, 8, 11, 14-18, 22-25, 28, 29 post onset, Kruskal-Wallis test) as the disease deteriorated (Fig. 2a), a trend that was also seen in $CD4^+$ and $CD8^+$ T cells (Fig. 2b-c). However, it was not found for NK ($CD16^+$, $CD56^+$) or B ($CD19^+$) cell (Fig. 2d-e).

We next compared the clinical parameters grouped by co-morbidity and found a significantly higher risk for disease progression if complicated by co-existing conditions (p=0.01, Extended Data Table 4), although the median age of co-morbidity group was also higher (p=0.02). Indeed, univariate logistic regression analysis indicated that age ($p<0.0001$), lymphocyte counts upon admission ($p<0.0001$), comorbidities (p=0.01) and gender (p=0.014) were the major factors associated with disease severity (Extended Data Table 5). Multivariate analysis showed that age (p=0.002) and lymphocytopenia (p=0.002) were two major independent factors whereas comorbidities did not reach to statistical significance.

The levels of eleven cytokines (IFN-α, IFN-γ, IL-1β, IL-2, IL-4, IL-5, IL-6, IL-8, IL-10, IL-12 and IL-17) in serum were measured upon admission and during treatment. Among them, IL-6 ($p<10^{-6}$) and IL-8 ($p=1\times10^{-5}$, Extended Data Table 3) showed most significant changes. Notably, these two cytokines exhibited an inverse correlation with lymphocyte count (Fig. 3a-b, Extended Data Table 5). Furthermore, we combined the longitudinal cytokine data of each group and plotted their fluctuation patterns against the time point post onset. We aggregated the highest IL-6 data from each patient from day 6 to 10 post onset and compared critical patients with non-critical ones. A significant higher IL-6 level in critical group was found (p=0.001, two-sided Mann-Whitney U test, Fig. 3c). A similarly significant difference was observed in the IL-8 level when aggregating data from day 16 to 20 post onset (p=0.006, Fig. 3d). These data suggest a strong link between inflammatory cytokines and pathogenesis of SARS-CoV-2 infection.

Discussion

Our analysis of some very recently treated patients provides further evidence that the viral genome is largely stable. In consistence with a recent study[8], we found that the observed small sequence variations divided the viral genomes into two major clades. We noticed that six sequences recovered from patients with contact history to HSWM all fell into Clade I, whereas three genomes from patients diagnosed in the same period but without exposure to HSWM were clustered into Clade II. Thus, these two major haplotypes likely represent two lineages derived from a common ancestor that independently evolved in early December 2019 in Wuhan, only one of which (Clade I) was spawned within the HSWM where high density of stalls, vendors and customers might have facilitated human-to-human transmission. In consistence with this idea, epidemiological investigations on the earliest cases in Wuhan before Dec. 18th identified two patients linked but five not linked to HSWM[4]. Our time-resolved phylogeny analysis suggests that the earliest zoonotic spillover event might occur at late November 2019, which is in agreement with the analysis by Andersen *et al*[8].

Nevertheless, patients infected with clade I or II virus did not exhibit significant difference in a suite of clinical features, mutation rate or transmissibility. Our data are in agreement with a lack of selection against either clade as suggested by others[9] but is at odds with the conclusion made by Tang et al, whose L/S type classification was based on the same two linked polymorphisms[10]. The presumed difference in transmissibility might be due to sampling bias, since the early uploaded sequences in the GISAID database were recovered from a limited number of critically ill patients and duplicate assemblies from the same patients were not uncommon[1,2,11].

Recently, Guan et al analyzed 1099 cases of COVID-19 in China and found lymphocytopenia to be one of the most common features in laboratory tests[5]. In this study, we confirmed this observation and further

found that $CD3^+$ T cell was the major cell type suppressed in infected patients, whereas $CD19^+$ B cell and $CD16^+CD56^+$ NK cells exhibited less suppression. Indeed, lymphopenia and in particular, reduced CD4/CD8 cell counts, were also major manifestation of SARS-CoV-2 infection[12]. Furthermore, our longitudinal monitoring of major cytokines indicated that IL-6 and IL-8 were negatively correlated with lymphocyte count and IL-6 kinetics was highly related to disease severity. At present, the relationships between virological activity, cytokine release and lymphocytopenia remain unclear. We hypothesize that the immunopathological response against SARS-CoV-2 involving "cytokine storm" and loss of $CD3^+$ T lymphocytes could constitute, at least in part, an underlying mechanism for disease progression and fatality. The macrophages in the lung could serve as the first driver of the "cytokine storm" in early phase of COVID-19 pneumonia[13] and subsequent lymphocyte infiltration mobilized by the cytokines, as observed in infected patients[14,15] and Rhesus Macaques[16], may explain the lymphocytopenia, although probable cytokine-induced T cell depletion could not be ruled out.

In conclusion, by closely monitoring the molecular and immunological data in 326 cases of COVID-19 patients, we suggest that adverse outcome is associated with depletion of $CD3^+$ T lymphocytes that is tightly linked to bursts of cytokines such as IL-6 and IL-8. Targeted sequencing of 94 cases infected during late-January to February indicated limited variations in the viral genome suggestive of a stable evolution. Two major lineages of the virus derived from one common ancestor may have originated independently from Wuhan in Dec 2019 and contributed to the current pandemic, although no major difference in clinical manifestation or transmissibility was found between them. Our data provide further evidence for the respective roles played by the viral and host factors in disease mechanism and underscore the importance of early intervention in therapy.

Online content

Any methods, additional references, Nature Research reporting summaries, source data, extended data, supplementary information, acknowledgements, peer review information; details of author contributions and competing interests; and statements of data and code availability are available at https://doi.org/10.1038/s41586-020-2355-0.

1. Zhu, N. *et al*. A Novel Coronavirus from Patients with Pneumonia in China, 2019. *N Engl J Med* **382**, 727-733, https://doi.org/10.1056/NEJMoa2001017 (2020).
2. Zhou, P. *et al*. A pneumonia outbreak associated with a new coronavirus of probable bat origin. *Nature* **579**, 270-273, https://doi.org/10.1038/s41586-020-2012-7 (2020).
3. Lam, T. T. *et al*. Identifying SARS-CoV-2 related coronaviruses in Malayan pangolins. *Nature*, https://doi.org/10.1038/s41586-020-2169-0 (2020).
4. Li, Q. *et al*. Early Transmission Dynamics in Wuhan, China, of Novel Coronavirus-Infected Pneumonia. *N Engl J Med* **382**, 1199-1207, https://doi.org/10.1056/NEJMoa2001316 (2020).
5. Guan, W. J. *et al*. Clinical Characteristics of Coronavirus Disease 2019 in China. *N Engl J Med*, https://doi.org/10.1056/NEJMoa2002032 (2020).
6. Chan, J. F. *et al*. A familial cluster of pneumonia associated with the 2019 novel coronavirus indicating person-to-person transmission: a study of a family cluster. *Lancet* **395**, 514-523, https://doi.org/10.1016/S0140-6736(20)30154-9 (2020).
7. Lu, R. *et al*. Genomic characterisation and epidemiology of 2019 novel coronavirus: implications for virus origins and receptor binding. *Lancet* **395**, 565-574, https://doi.org/10.1016/S0140-6736(20)30251-8 (2020).
8. Andersen, K. G., Rambaut, A., Lipkin, W. I., Holmes, E. C. & Garry, R. F. The proximal origin of SARS-CoV-2. *Nat Med* **26**, 450-452, https://doi.org/10.1038/s41591-020-0820-9 (2020).
9. MacLean, O. A., Orton, R., Singer, J. B. & Robertson, D. L. Response to "On the origin and continuing evolution of SARS-CoV-2". *http://virological.org/t/response-to-on-the-origin-and-continuing-evolution-of-sars-cov-2/418* (2020).
10. Tang, X. *et al*. On the origin and continuing evolution of SARS-CoV-2. *National Science Review*, https://doi.org/10.1093/nsr/nwaa036 (2020).
11. Ren, L. L. *et al*. Identification of a novel coronavirus causing severe pneumonia in human: a descriptive study. *Chin Med J (Engl)*, https://doi.org/10.1097/CM9.0000000000000722 (2020).
12. Wong, R. S. *et al*. Haematological manifestations in patients with severe acute respiratory syndrome: retrospective analysis. *BMJ* **326**, 1358-1362, https://doi.org/10.1136/bmj.326.7403.1358 (2003).
13. Tian, S. *et al*. Pulmonary Pathology of Early-Phase 2019 Novel Coronavirus (COVID-19) Pneumonia in Two Patients With Lung Cancer. *J Thorac Oncol*, https://doi.org/10.1016/j.jtho.2020.02.010 (2020).
14. Xu, Z. *et al*. Pathological findings of COVID-19 associated with acute respiratory distress syndrome. *Lancet Respir Med* **8**, 420-422, https://doi.org/10.1016/S2213-2600(20)30076-X (2020).
15. Wang, C. *et al*. Aveolar Macrophage Activation and Cytokine Storm in the Pathogenesis of Severe COVID-19. https://doi.org/10.21203/rs.3.rs-19346/v1 (2020).
16. Shan, C. *et al*. Infection with Novel Coronavirus (SARS-CoV-2) Causes Pneumonia in the Rhesus Macaques. https://doi.org/10.21203/rs.2.25200/v1 (2020).

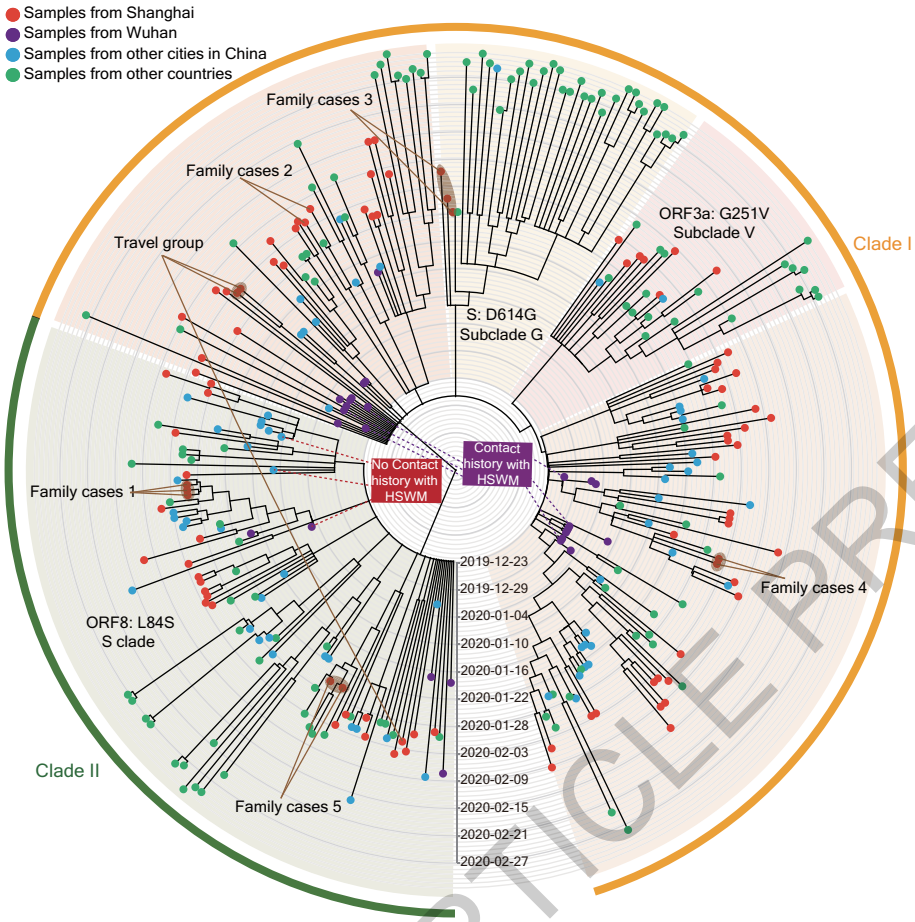

Fig. 1 | Phylogenetic analysis of the assembled SARS-CoV-2 genomes. A total of 94 SARS-CoV-2 genome sequences and 221 published sequences were used for construction of time-resolved phylogeny tree. Clades I and clade II are marked and variations distinguishing branches of the phylogeny tree were indicated. Concentric circles at the graph represent time scale of sampling date. Each tip circle stands for a single sample, while the colors marks case locations (red represent Shanghai, purple represents Wuhan, blue represents other cities in China, and green represents other countries and districts). Cases related to HSWM are highlighted.

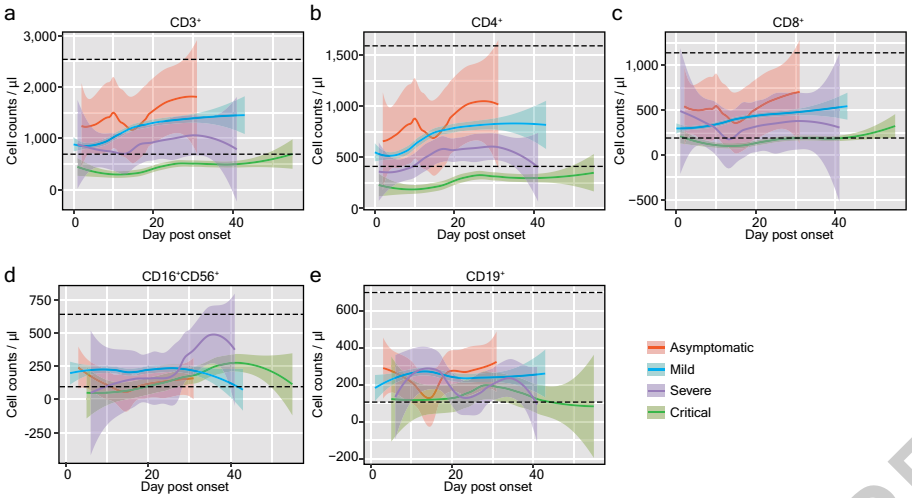

Fig. 2 | Temporal changes of CD3$^+$ (a), CD4$^+$ (b), CD8$^+$ (c), CD16$^+$CD56$^+$ (d) and CD19$^+$ (e) cell counts in each group during hospitalization. The median values of each time-point (day from onset) were shown. The 95% interval was plotted as colored shadow. The normal range of each cell type was plotted as dotted lines. (a-c: n=325, d-e: n=220).

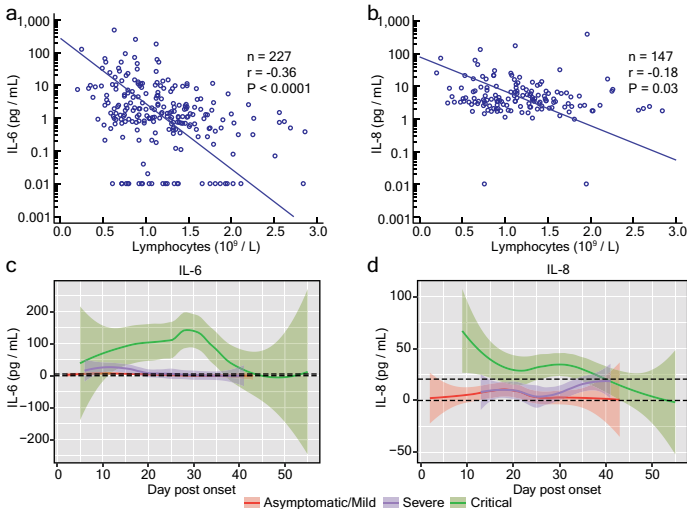

Fig. 3 | Correlation between inflammatory cytokines and lymphocyte counts. The levels of serum IL-6 (**a**) and IL-8 (**b**) upon admission were plotted against lymphocyte count. Two-sided Spearman's correlation analysis with no adjustment of multiple comparisons was performed. Temporal changes of IL-6 (**c**, n=230) and IL-8 (**d**, n=149) in each group during hospitalization were shown. The median values of each time-point (day from onset) were shown. The 95% interval was plotted as colored shadow. The normal range of each cytokine was plotted as dotted lines.

Methods

Ethics statement

This study was approved by the Shanghai Public Health Clinical Center Ethics Committee (No. YJ-2020-S015-01). Informed consents had been obtained from all the enrolled patients.

Patients

A total of 326 patients, who were tested positive for SARS-CoV-2 RNA and were admitted into Shanghai Public Health Clinical Center from Jan 20th to Feb 25th, which was the designated hospital receiving all the COVID-19 cases in Shanghai, were included in this study. In addition to routine clinical tests, measurement of serum cytokine was performed on 228 patients. Their basic demographic, epidemiological and clinical characteristics were shown in Extended Data Table 1. The median age of the patients was 51 years (range 15-88) with a male: female sex ratio of 1.10. Among these 326 patients, 125 (38.34%) had at least one comorbidity, the most common were hypertension (76 cases), diabetes (24 cases), coronary heart disease (13 cases), chronic hepatitis B (10 cases), chronic obstructive pulmonary disease (2 cases), chronic renal disease (2 cases) and cancer (3 cases). The disease severity was categorized into four stages, i.e., asymptomatic, mild, severe and critical, according to the Guidelines on the Diagnosis and Treatment of Novel Coronavirus issued by the National Health Commission, China (7th edition). Briefly, asymptomatic disease was defined as normal body temperature, lack of respiratory symptoms and no pulmonary radiological manifestation, mild disease was defined as having fever, respiratory symptoms and radiological evidence of pneumonia. Severe cases were defined by meeting one of the following manifestations: respiratory rate > 30/min, oxygen saturation levels (SpO2) <93%, arterial partial pressure of oxygen (PaO2)/fraction of inspired oxygen (FiO2)(PaO2/FiO2 ratio) <=300mmHg or pulmonary imaging shows multi-lobular lesions or lesion progression exceeding 50% within 48 hours. Critical condition was defined as one of the following: acute respiratory distress syndrome requiring mechanical ventilation, shock, complications with other organ failure.

Nucleic acid extraction, molecular screening and genome sequencing

Swabs and sputum samples were collected for nucleic acid extraction using automatic magnetic extraction device and accompanying kit (Shanghai Bio-Germ) and screened with a semi-quantitative RT-PCR kit (Shanghai Bio-Germ) with amplification targeting the ORF1a/b and N gene. Deep sequencing was done using the nucleic acid extracted from the RT-PCR confirmed cases hospitalized in Shanghai Public Health Clinical Center. We used a multiplexed amplicon strategy as described[17] the primers were synthesized as described (https://github.com/artic-network/artic-ncov2019/blob/master/primer_schemes/nCoV-2019/V1/nCoV-2019.tsv). The primers were split into 10 subpools each containing 9-10 pairs for specific amplification of 400bp viral sequence using the remaining cDNA from the diagnostic test. The PCR amplicons were purified using AMPure DNA cleanup steps. The amplicon libraries were generated using a NanoPrep for Illumina kit (IDT) according to the manufacturer's instructions. Briefly, the procedures included end-repair, 3' ends adenylation, adapter ligation and PCR amplification, followed by assessing DNA library quality. Amplicon sequencing was performed with established Illumina protocols on MiSeq platform (Illumina) according to a 2×300 bp protocol in the National Research Center for Translational Medicine (Shanghai).

Viral genomic sequence variation calling

All clean reads were mapped to the SARS-CoV-2 genome (Wuhan-Hu-1, GenBank accession no. MN908947) using BWA (version 0.7.17)[18]. Variations were called with mpileup tools in samtools[19]. Low-quality variations that depth lower than 10 and Qual score lower than 50 were filtered by bcftools (version 1.9).

Phylogenetic analysis

Sequencing reads were trimmed with Trimmomatic (version 0.39)[20] to remove low quality region, adapter sequences and sequencing primers. Clean reads were used to build virus genome assemblies with VirGenA (version 1.4)[21]. A post-assembly procedure was manually performed to remove low quality content and potential sequencing artifacts. 94 assemblies with coverage above 90% were qualified for phylogeny analysis. MAFFT (version 7.453)[22] made the multi-sequence alignment after trimming off N's on both ends of the genome sequences. The computation and visualization platform used for the phylogeny analysis is Nextstrain (version 1.15.0)[23]. The module we selected for phylogenetic tree building is IQ-TREE (version 1.6.12)[24]. An automatic substitution model selection was performed and the TIM+F+I model was selected to build the Maximum Likelihood phylogeny tree based on Bayesian information criteria (BIC) score. TreeTime (version 0.7.3)[25] was used for time resolved phylogeny analysis. The resulting phylogeny tree was visualized by auspice from Nextstrain package. All bioinformatics analyses were performed using the ASTRA supercomputing platform (Sugon, China) with Optane memory technology in the National Research Center for Translational Medicine (Shanghai).

Cytokine quantification and lymphocyte subset counting

Becton-Dickinson (BD) cytometric bead array (human Th1/Th2/Th17 cytokine kit and Human Inflammatory Cytokine Kit) was used quantify serum cytokines (IFN-α, IFN-γ, IL-1β, IL-2, IL-4, IL-5, IL-6, IL-8, IL-10, IL-12 and IL-17). $CD3^+$ T, $CD4^+$ T and $CD8^+$ T, $CD19^+$ B, and $CD16^+CD56^+$ natural killer (NK) cells were stained using BD Multitest™ 6-color TBNK reagent in Trucount tubes and analyzed using the BD FACSCanto™ II flow cytometer. The longitudinal plots of cytokines and cell count data were visualized using the geom_smooth tool in the ggplot2 R package.

Statistical analysis

Two sided Mann-Whitney U test and Kruskal Wallis test were used to compare two and more than two groups of variables. Chi square and Fisher's exact test was used for analyzing contingency tables. Spearman's rank correlation test was used to evaluate correlations.

Reporting summary

Further information on research design is available in the Nature Research Reporting Summary linked to this paper.

Data availability

The 94 genome sequences with over 90% coverage were deposited to GISAID (EPI_ISL_416316-EPI_ISL_416409) and the phylogeny result is accessible via web address http://ncov.linc.org.cn. The amplicon sequencing reads for variant calling were deposited to NCBI Bioproject (PRJNA627662) and NODE (http://www.biosino.org/node/project/detail/OEP000877).

17. Quick, J. *et al*. Multiplex PCR method for MinION and Illumina sequencing of Zika and other virus genomes directly from clinical samples. *Nat Protoc* **12**, 1261-1276, https://doi.org/10.1038/nprot.2017.066 (2017).
18. Li, H. & Durbin, R. Fast and accurate short read alignment with Burrows-Wheeler transform. *Bioinformatics* **25**, 1754-1760, https://doi.org/10.1093/bioinformatics/btp324 (2009).
19. Li, H. *et al*. The Sequence Alignment/Map format and SAMtools. *Bioinformatics* **25**, 2078-2079, https://doi.org/10.1093/bioinformatics/btp352 (2009).
20. Bolger, A. M., Lohse, M. & Usadel, B. Trimmomatic: a flexible trimmer for Illumina sequence data. *Bioinformatics* **30**, 2114-2120, https://doi.org/10.1093/bioinformatics/btu170 (2014).
21. Fedonin, G. G., Fantin, Y. S., Favorov, A. V., Shipulin, G. A. & Neverov, A. D. VirGenA: a reference-based assembler for variable viral genomes. *Brief Bioinform* **20**, 15-25, https://doi.org/10.1093/bib/bbx079 (2019).

22. Katoh, K. & Standley, D. M. MAFFT multiple sequence alignment software version 7: improvements in performance and usability. *Mol Biol Evol* **30**, 772-780, https://doi.org/10.1093/molbev/mst010 (2013).
23. Hadfield, J. *et al*. Nextstrain: real-time tracking of pathogen evolution. *Bioinformatics* **34**, 4121-4123, https://doi.org/10.1093/bioinformatics/bty407 (2018).
24. Nguyen, L. T., Schmidt, H. A., von Haeseler, A. & Minh, B. Q. IQ-TREE: a fast and effective stochastic algorithm for estimating maximum-likelihood phylogenies. *Mol Biol Evol* **32**, 268-274, https://doi.org/10.1093/molbev/msu300 (2015).
25. Sagulenko, P., Puller, V. & Neher, R. A. TreeTime: Maximum-likelihood phylodynamic analysis. *Virus Evol* **4**, vex042, https://doi.org/10.1093/ve/vex042 (2018).

Acknowledgements This work is supported by National Megaprojects of China for Infectious Diseases (2017ZX10103009-001, 2018ZX10305409-001-005); Double First-class project of Fudan University (No.IDF162005) and the Scientific research for special subjects on 2019 novel coronavirus of Shanghai Public Health Clinical Center (No.2020YJKY01). Double First-Class Project (WF510162602) from the Ministry of Education, State Key Laboratory of Medical Genomics, Overseas Expertise Introduction Project for Discipline Innovation (111 Project, B17029) and National Key R&D Program of China (2019YFA0905902), the Shanghai Guangci Translational Medical Research Development Foundation. We acknowledge all healthcare personnel involved in the diagnosis and treatment of patients in Shanghai Public Health Clinical Center, we thank Prof. Zhu Chen for guidance in study design, interpretation of results and critical revision of the manuscript. We are grateful to all the researchers who shared their SARS-CoV-2 genome sequences in GISAID. This manuscript is dedicated to Prof. Yunwen Hu of Shanghai Public Health Clinical Center, whose life-long commitment to infectious disease research would never be forgotten.

Author contributions S.C., H.L., XN.Z., S.W. Z.Y. conceived the study. XN.Z., Y.L., Z.Y., X.J., M.W., B.S., S.X., J.C., W.W. collected the patient samples, epidemiological and clinical data, XN.Z., X.J., M.W. processed viral RNA isolation and PCR, S.Y., J.L., L.J., G.L., J.W. performed sequencing and sequence assembly. XN.Z., Y.T., F.L., G.L., B.S., S.X., J.C., B.C., M.X., S.W., S.C. carried out data acquisition, analysis, and interpretation. XN.Z., Y.T., F.L., G.L. drafted the manuscript. S.C., S.W., XX.Z., G.Z. revised the final manuscript.

Competing interests The authors declare no competing interests.

Additional information
Supplementary information is available for this paper at https://doi.org/10.1038/s41586-020-2355-0.
Correspondence and requests for materials should be addressed to S.W., S.C. and H.L.
Peer review information *Nature* thanks Luke O'Neill and the other, anonymous, reviewer(s) for their contribution to the peer review of this work.
Reprints and permissions information is available at http://www.nature.com/reprints.

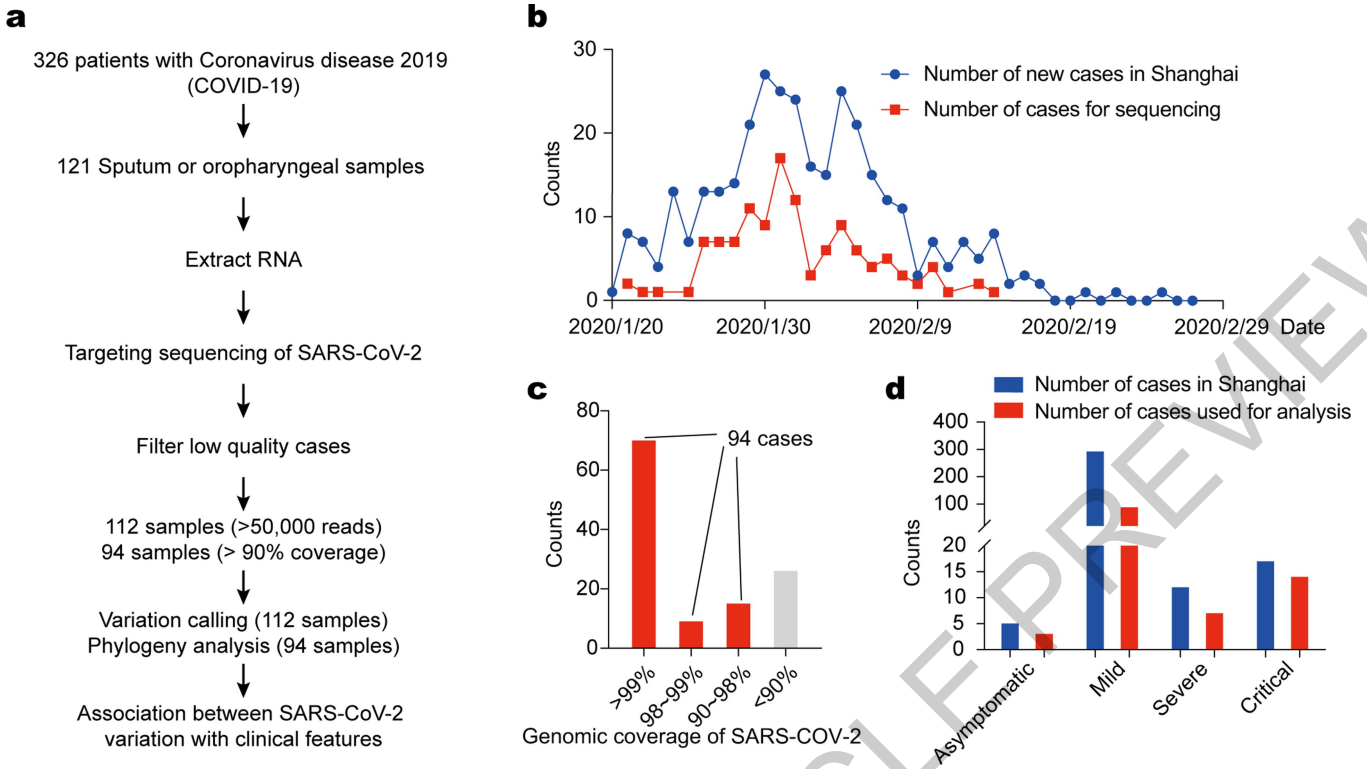

Extended Data Fig. 1 | High-throughput targeting sequencing process. **a**, Design of experiment and analysis pipeline. A total of 121 samples, including sputum, oropharyngeal swab samples from COVID-19 patients, were used for viral RNA extraction and sequencing. **b**, Comparison of COVID-19 cases used for sequencing with total cases in the Shanghai cohort between 20th Feb and 25th Jan 2020. **c**, Bar plot of the coverage of SARS-CoV-2 genome per sample in four bins, i.e. >99%, 98-99%, 90-98%, and <90%. 94 samples have coverages of over 90%. **d**, Numbers of severe/critical and mild/asymptomatic COVID-19 cases. Blue bar represents number of cases included in this study. Red bar represents number of cases used for variant calling or phylogeny analysis.

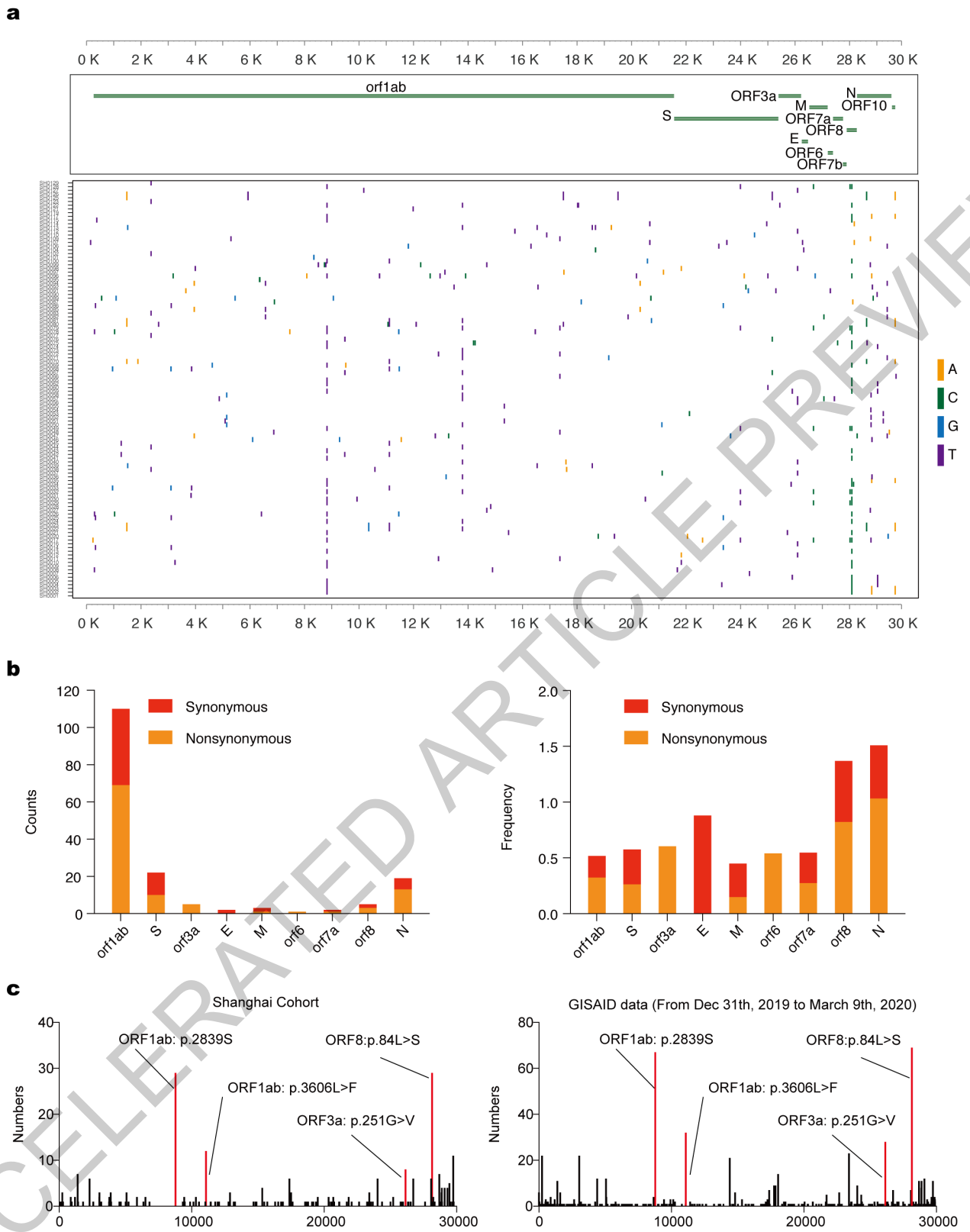

Extended Data Fig. 2 | Characteristics of single nucleotide variations in 112 Shanghai SARS-CoV-2. a, Frequencies of variations in Shanghai cohort and published GISAID dataset. **b**, Summary of 169 variations in nine open reading frames. Variation counts and the ratio of synonymous/nonsynonymous mutations were plotted. Black represents synonymous; orange represents nonsynonymous. **c**, Single nucleotide variations between the SARS-CoV-2 reference genome (Wuhan-Hu-1) and genome sequences in the Shanghai cohort were shown by vertical color bars. Orange: A, Blue: G, Green: C, Purple: T. The upper panel shows the open reading frame of each gene.

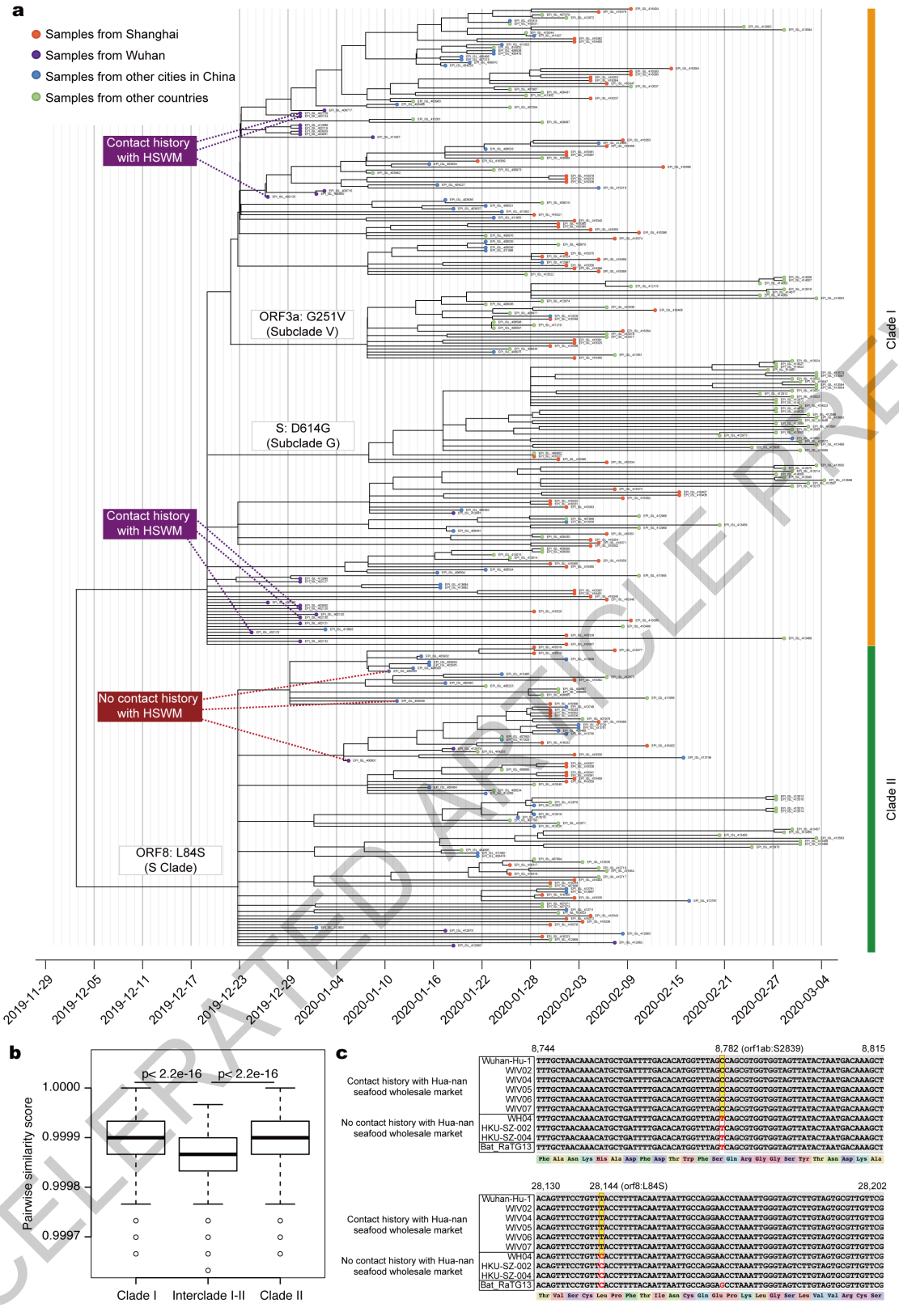

Extended Data Fig. 3 | See next page for caption.

Extended Data Fig. 3 | Phylogenetic analysis of the assembled SARS-CoV-2 genomes. a, A total of 94 SARS-CoV-2 genome sequences and 221 published sequences (same as Fig. 1a) were used for construction of time-resolved rectangular phylogeny tree. Clade I and clade II are marked, and variations distinguishing branches of the phylogeny tree were indicated. Each tip circle represents a single sample. The position of each sample along the X-axis corresponds to the sample collection date. Case locations are marked by colors (red represent Shanghai, purple represents Wuhan, blue represents other cities in China, and green represents other countries and districts). GISAID accession IDs are displayed alongside each tip circle. Cases with or without contact history to HSWM are highlighted. **b**, Boxplot (centre, median; box, interquartile range (IQR); whiskers, 1.5 × IQR) of pairwise similarity scores within Clade I (n=22,791), Interclade I-II (n=21,614) and Clade II (n=5,050) were depicted. The two-sided unpaired t-test was used for statistical analysis. **c**, Alignment of sequences around nucleotides 8782 and 28144 using Bat-SARS-CoV-RaTG13 and SARS-CoV-2 sequences recovered from patients with known history of exposure to HSWM.

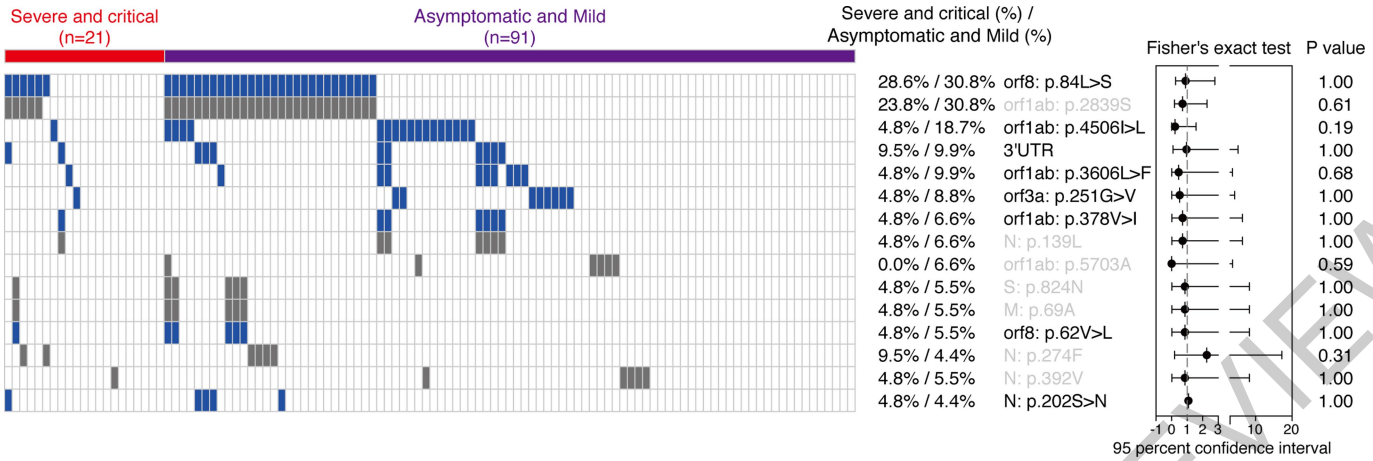

Extended Data Fig. 4 | SARS-CoV-2 variation in severe/critical and mild cases of COVID-19. Variations of SARS-CoV-2 in different categories of COVID-19 patients were plotted. Blued boxes indicate nonsynonymous mutations; gray boxes indicate synonymous mutations. Red bars represent the severe and critical COVID-19 group and the purple bar represents the mild COVID-19 group. Two-sided Fisher's exact test was used for determining the statistical significance. The 95% confidence interval and odds ratios were plotted. P values and their 95% confidence intervals were shown on the right.

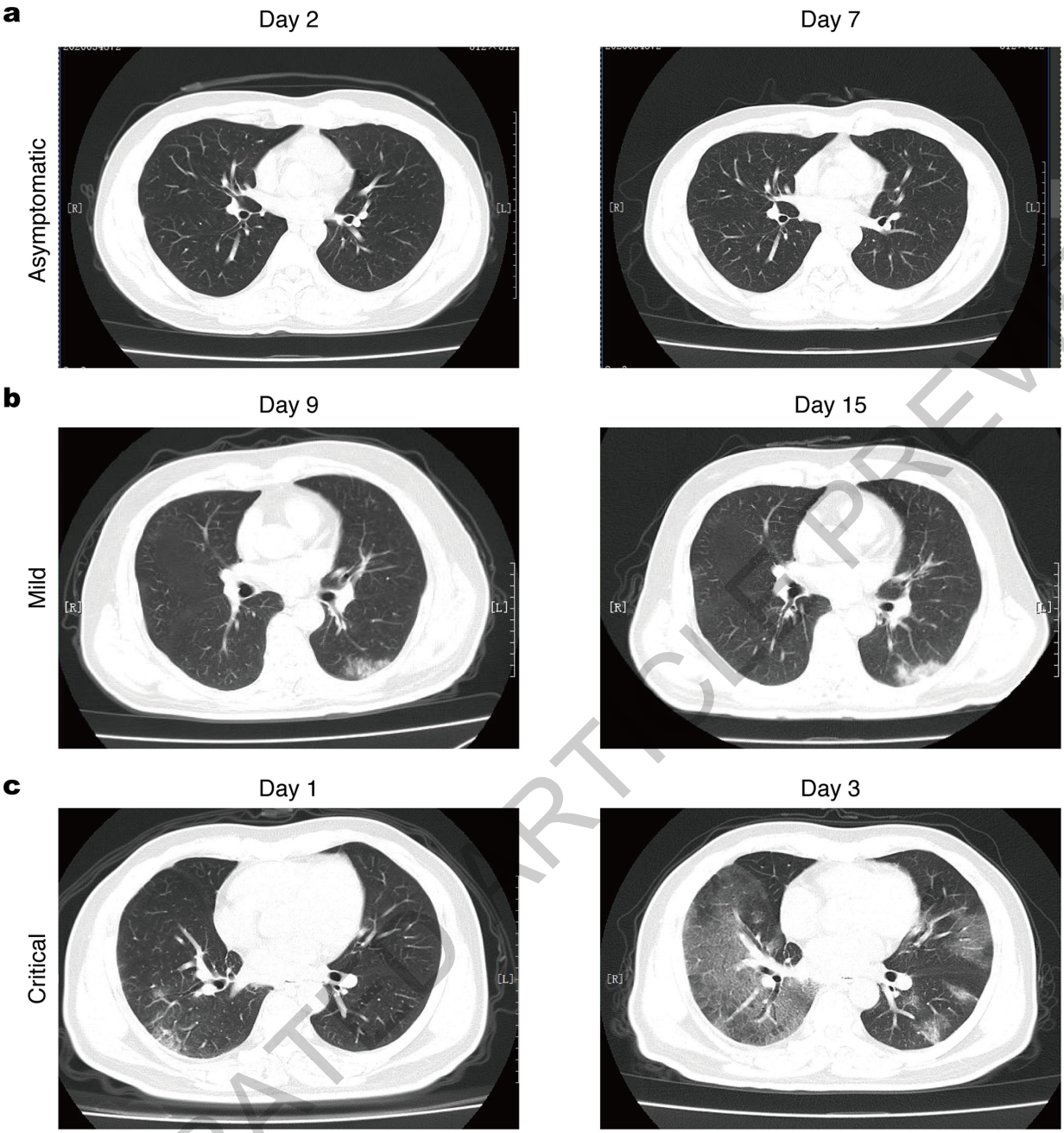

Extended Data Fig. 5 | Computed tomographic scans of three typical patients (a, asymptomatic, b, mild and c, critical) during hospitalization. The respective time-point (day post admission) of the examination was shown. The computed tomography scans were performed once for each patient on a specific date during treatment. Images from 5 asymptomatic, 7 mild and 13 critical cases were analyzed. Typical images from each group were shown.

Extended Data Table 1 | Clinical features of enrolled patients and subgroups

	Entire cohort (n=326)	Phylogeny (n=94)	Cytokine analysis (n=228)
Age			
Median (range)-year	51 (15-88)	53 (24-85)	53.5 (21-85)
<=39 --no. (%)	109 (33.44%)	32 (34.04%)	75 (32.89%)
40-49 --no. (%)	49 (15.03%)	10 (10.64%)	25 (10.96%)
50-59 --no. (%)	55 (16.87%)	18 (19.15%)	40 (17.54%)
60-69 --no. (%)	80 (24.54%)	22 (23.40%)	63 (27.63%)
>=70 --no. (%)	33 (10.12%)	12(12.76%)	25 (10.96%)
Gender			
Female (%)	155(47.54%)	44 (46.81%)	110 (48.24%)
Male (%)	171 (52.46 %)	50 (53.19%)	118 (51.75%)
Exposure to source of transmission within 14 days			
Local residents of Hubei --no. (%)	90 (27.60%)	26 (27.66%)	56 (24.56%)
Recently been to Hubei --no. (%)	80 (24.54%)	25 (26.60%)	47 (20.61%)
Contacted with people from Hubei --no. (%)	52 (15.96%)	14 (14.89%)	45 (19.74%)
Other or unknown --no. (%)	104 (31.90%)	29 (30.85%)	80 (35.09%)
Highest Temperature (°C)	38.0 (36.6 -40.0)	38.2 (36.6-40.0)	38.0 (36.0-40.0)
Disease Severity			
Asymptomatic --no. (%)	5 (1.53%)	0 (0)	3 (1.32%)
Mild --no. (%)	293 (89.88%)	78 (82.98%)	200 (87.72%)
Severe –no. (%)	12 (3.68%)	5 (5.32%)	10 (4.39%)
Critical –no. (%)	16 (4.91%)	11 (11.70%)	15 (6.58%)
Death --no. (%)	6 (1.84%)	5 (5.32%)	5 (2.19%)
Any Co-morbidities	125 (38.34)	38 (40.42%)	90 (39.47%)
Hypertension --no. (%)	76 (23.31%)	24 (25.53%)	60 (26.32%)
Diabetes --no. (%)	24 (9.13%)	9 (9.57%)	18 (7.89%)
Coronary heart disease --no. (%)	13 (3.99%)	5 (5.32%)	7 (3.07%)
Chronic hepatitis B --no. (%)	10 (3.07%)	5 (5.32%)	4 (1.75%)
Chronic obstructive pulmonary disease –no. (%)	2 (0.61%)	1 (1.06%)	1 (0.44%)
Chronic renal diseases --no. (%)	2 (0.61%)	1 (1.06%)	1 (0.44%)
Cancer --no. (%)	3 (0.92%)	2 (2.13%)	2 (0.88%)

Extended Data Table 2 | Clinical features of different clades of SARS-CoV-2

	Clade I (n=78)	Clade II (n=34)	P value
Age-year	57.5 (41-65)	46.5 (32-62)	0.02 [a]
Disease status			
Critical	10	4	
Non-critical	68	30	0.88 [b]
Leukocytes counts (×10^9/L, normal range 3.5-9.5)	4.46 (3.80-5.66)	4.80 (4.11-5.65)	0.58 [a]
Lymphocytes (× 10^9/L, normal range 1·1–3·2)	1.07 (0.76-1.40)	1.01 (0.71-1.37)	0.79 [a]
CD3+T cell counts (/μL, normal range 690-2540)	720 (503-943)	606 (411-854)	0.21 [a]
CD8+T cell counts (/μL, normal range 190-1140)	222 (164-371)	188 (135-283)	0.14 [a]
CD4+T cell counts (/μL, normal range 410-1590)	404 (279-608)	367 (219-578)	0.38 [a]
Platelets (×10^9/L, normal range 125-350)	158.5 (130-208)	178 (151-207)	0.18 [a]
Haemoglobin (g/L, 115-150)	137 (124-149)	141 (130-150)	0.22 [a]
C-reactive protein (mg/L, normal range 0.9-1.8)	13.35 (5.4-41.6)	18.35(5.67-32.4)	0.83 [a]
Lactose dehydrogenase (U/L, normal range 120-250)	221 (186-280)	240 (195-299)	0.23 [a]
Complement C3 (mg/L, normal range <3)	1.13 (1.01-1.29)	1.15 (1.01-1.29)	0.81 [a]
D-dimer (μg/L, normal range 0-0.5)	0.415 (0.30-0.71)	0.35 (0.25-0.57)	0.19 [a]
IL-6 (pg/ml, normal range <5.4 pg/ml)	1.46 (0.69-8.17)	2.12 (0.75-6.29)	0.92 [a]
IL-8 (pg/ml, normal range <20.6 pg/ml)	4.72 (3.41-6.03)	3.40 (2.61-7.03)	0.32 [a]
Duration of virus shedding after onset (days)	16 (11-24)	18 (12-24)	0.79 [a]

Data are presented as median (IQR); a, two-sided Mann-Whitney U test, b, Chi-square test

Extended Data Table 3 | Immunological and biochemical parameters associated with disease severity

	Asymptomatic (n=5)	Mild (n=293)	Severe (n=12)	Critical (n=16)	P value*
Leukocytes counts ($\times10^9$/L, normal range 3.5-9.5)	7.13 (4.03-8.72)	4.83 (4.03-5.89)	4.30 (3.53-7.76)	5.52 (4.12-7.74)	0.30
Lymphocytes ($\times 10^9$/L, normal range 1·1–3·2)	1.59 (1.23-2.08)	1.25 (0.85-1.49)	0.91 (0.66-1.40)	0.64 (0.44-0.88)	6×10^{-6}
$CD3^+$T cell count (/μL,normal range 690-2540)	1208(1012-1591)	778 (553-1041)	500 (379-705)	234 (152-474)	$<1\times10^{-6}$
$CD8^+$T cell count (/μL, normal range 190-1140)	495 (405-615)	265 (171-393)	133 (102-199)	96 (52-211)	1×10^{-5}
$CD4^+$T cell count (/μL, normal range 410-1590)	634 (529-909)	455 (314-650)	332 (226-541)	130 (96-254)	$<1\times10^{-6}$
Platelets ($\times10^9$/L, normal range 125-350)	187 (165-219)	182 (145-225)	162 (130-198)	156 (119-202)	0.23
$CD19^+$ B cell counts (/μL, normal range 107-698)	289 (223-320)	228 (160-309)	221 (108-269)	111 (58-135)	1×10^{-5}
$CD16^+CD56^+$ NK cells (/μL, normal range 95-640)	160 (102-219)	188 (130-267)	170 (113-279)	82 (41-174)	0.04
Haemoglobin (g/L, 115-150)	139 (132-147)	135 (126-148)	142 (126-146)	145 (126-150)	0.71
C-reactive protein (mg/L, normal range 0.9-1.8)	<3	11.4 (3.9-25.2)	46.1 (17.4-92.8)	71.2 (37.0-120.0)	$<1\times10^{-6}$
Alanine aminotransferase (U/L, normal range 7-40)	17 (9-24.3)	21 (15-32)	29 (20-37)	27 (17.5-33.0)	0.16
Lactose dehydrogenase (U/L, normal range 120-250)	174 (162-180)	225 (193-269)	355 (309-401)	371 (293-460)	$<1\times10^{-6}$
Complement C3 (mg/L, normal range <3)	1.02 (0.92-1.06)	1.17 (1.04-1.30)	1.19 (0.99-1.32)	1.00 (0.86-1.28)	0.03
D-dimer (μg/L, normal range 0-0.5)	0.3 (0.2-0.4)	0.4 (0.3-0.7)	0.7 (0.5-1.6)	0.8 (0.5-1.3)	2×10^{-5}
IL-6 (pg/ml, normal range <5.4 pg/ml)	0.3 (0.1-5.7)	1.1 (0.5-3.2)	6.0 (1.1-11.1)	33.0 (9.0-110.6)	$<1\times10^{-6}$
IL-8 (pg/ml, normal range <20.6 pg/ml)	7.2 (3.1-7.3)	3.5 (2.3-6.0)	8.1 (3.6-16.8)	21.4 (7.2-58.7)	1×10^{-5}

*Kruskal-Wallis test. Data are presented as median (IQR)

Extended Data Table 4 | Clinical features of patients with and without co-morbidities

Co-morbidities	No (n=201)	Yes (n=125)	P value
Age-year	48 (35-63)	54 (39-66)	0.02 [a]
Disease status			
Critical	5	11	
Non-critical	196	114	0.01 [b]
Leukocytes counts (×10^9/L, normal range 3.5-9.5)	4.70 (3.91-5.93)	5.01 (4.10-6.02)	0.34 [a]
Lymphocytes (× 10^9/L, normal range 1·1–3·2)	1.13 (0.81-1.49)	1.12 (0.77-1.48)	0.65 [a]
$CD3^+$T cell counts (/μL, normal range 690-2540)	752 (504-1023)	716 (497-1042)	0.58 [a]
$CD8^+$T cell counts (/μL, normal range 190-1140)	259 (171-396)	257 (143-386)	0.40 [a]
$CD4^+$T cell counts (/μL, normal range 410-1590)	448 (301-633)	415 (306-651)	0.67 [a]
Platelets (×10^9/L, normal range 125-350)	179 (145-224)	178 (142-221)	0.65 [a]
Haemoglobin (g/L, 115-150)	136 (127-148)	135 (125-149)	0.87 [a]
C-reactive protein (mg/L, normal range 0.9-1.8)	11.05 (3.0-22.9)	16.2 (4.98-49.8)	0.005 [a]
Lactose dehydrogenase (U/L, normal range 120-250)	225 (192-277)	239 (199-303)	0.11 [a]
Complement C3 (mg/L, normal range <3)	1.13 (1.01-1.29)	1.23 (1.08-1.30)	0.04 [a]
D-dimer (μg/L, normal range 0-0.5)	0.41 (0.29-0.70)	0.45 (0.29-0.84)	0.21 [a]
IL-6 (pg/ml, normal range <5.4 pg/ml)	1.09 (0.45-4.28)	1.51 (0.74-8.50)	0.06 [a]
IL-8 (pg/ml, normal range <20.6 pg/ml)	3.71 (2.58-6.72)	5.25 (2.30-9.17)	0.36 [a]
Onset to hospitalization (day)	4 (2-7)	4 (2-7.5)	0.62
Duration of virus shedding after onset (days)	15 (10-20)	15 (10-21.25)	0.33 [a]

Data are presented as median (IQR); a, two-sided Mann-Whitney U test, b, Chi-square test

Extended Data Table 5 | Univariate and multivariate logistic regression analyses of factors associated with disease severity

Clinical Variables *	Odds Ratio	95% CI		P value
		Lower	Upper	
UNIVIARIATE ANALYAIS				
Age-year	1.128	1.07	1.19	<0.0001
Gender	0.221	0.067	0.858	0.014
Lymphocyte count	0.0099	0.0011	0.0899	<0.0001
$CD3^+$ T cell counts	0.9932	0.9901	0.9962	<0.0001
$CD4^+$ T cell counts	0.9878	0.9823	0.9932	<0.0001
$CD8^+$ T cell counts	0.9900	0.9840	0.9959	0.0003
$CD19^+$ B cell counts	0.9797	0.9703	0.9892	<0.0001
$CD16^+CD56^+$ NK cell counts	0.9949	0.9891	1.0007	0.045
IL-6	1.0623	1.0329	1.0926	<0.0001
IL-8	1.0133	0.9992	1.0276	0.0164
Comorbidity	3.40	1.29	11.20	0.01
MULTIVARIATE ANALYSIS				
Age-year	1.09	1.03	1.16	0.002
Lymphocyte count	0.03	0.003	0.273	0.002

*Critical cases (n=16) versus asymptomatic/mild/severe cases of COVID-19 (n=310).

nature research

Corresponding author(s): Hongzhou Lu, Saijuan Chen, Shengyue Wang

Last updated by author(s): Apr 23, 2020

Reporting Summary

Nature Research wishes to improve the reproducibility of the work that we publish. This form provides structure for consistency and transparency in reporting. For further information on Nature Research policies, see Authors & Referees and the Editorial Policy Checklist.

Statistics

For all statistical analyses, confirm that the following items are present in the figure legend, table legend, main text, or Methods section.

n/a	Confirmed
☐	☒ The exact sample size (*n*) for each experimental group/condition, given as a discrete number and unit of measurement
☐	☒ A statement on whether measurements were taken from distinct samples or whether the same sample was measured repeatedly
☐	☒ The statistical test(s) used AND whether they are one- or two-sided *Only common tests should be described solely by name; describe more complex techniques in the Methods section.*
☒	☐ A description of all covariates tested
☐	☒ A description of any assumptions or corrections, such as tests of normality and adjustment for multiple comparisons
☐	☒ A full description of the statistical parameters including central tendency (e.g. means) or other basic estimates (e.g. regression coefficient) AND variation (e.g. standard deviation) or associated estimates of uncertainty (e.g. confidence intervals)
☐	☒ For null hypothesis testing, the test statistic (e.g. *F*, *t*, *r*) with confidence intervals, effect sizes, degrees of freedom and *P* value noted *Give P values as exact values whenever suitable.*
☒	☐ For Bayesian analysis, information on the choice of priors and Markov chain Monte Carlo settings
☒	☐ For hierarchical and complex designs, identification of the appropriate level for tests and full reporting of outcomes
☒	☐ Estimates of effect sizes (e.g. Cohen's *d*, Pearson's *r*), indicating how they were calculated

Our web collection on statistics for biologists contains articles on many of the points above.

Software and code

Policy information about availability of computer code

Data collection	Miseq control software (version 2.6.2.1)
Data analysis	Trimmomatic (version 0.39), BWA (version 0.7.17), Samtools (version 1.10), VirGenA (version 1.4), MAFFT (version 7.453), IQ-TREE (version 1.6.12), TreeTime (version 0.7.3), Nextstrain (version 1.15.0), R (version 3.6.2), ggplot2 (version 3.3.0), bcftools (version 1.9), Graphpad Prism (version 6), Medcalc (version 15).

For manuscripts utilizing custom algorithms or software that are central to the research but not yet described in published literature, software must be made available to editors/reviewers. We strongly encourage code deposition in a community repository (e.g. GitHub). See the Nature Research guidelines for submitting code & software for further information.

Data

Policy information about availability of data

All manuscripts must include a data availability statement. This statement should provide the following information, where applicable:

- Accession codes, unique identifiers, or web links for publicly available datasets
- A list of figures that have associated raw data
- A description of any restrictions on data availability

The 94 genome sequences with over 90% coverage were deposited to GISAID (EPI_ISL_416316-- EPI_ISL_416409). The phylogeny result is accessible via web address http://ncov.linc.org.cn. The amplicon sequencing reads for variant calling were deposited to NCBI Bioproject (PRJNA627662).

Field-specific reporting

Please select the one below that is the best fit for your research. If you are not sure, read the appropriate sections before making your selection.

☒ Life sciences ☐ Behavioural & social sciences ☐ Ecological, evolutionary & environmental sciences

For a reference copy of the document with all sections, see nature.com/documents/nr-reporting-summary-flat.pdf

Life sciences study design

All studies must disclose on these points even when the disclosure is negative.

Sample size	A total of 326 patients, who were tested positive for SARS-CoV-2 RNA and were admitted into Shanghai Public Health Clinical Center from Jan 20th to Feb 25th were included. In addition to routine clinical tests, measurement of serum cytokine was performed on 228 patients. Phylogenetic analysis was performed on genome sequences (>90% complete) recovered from 94 patients. The sample size was determined by the maximum available clinical and laboratory information in our center. No prior sample size calculation was performed.
Data exclusions	No data excluded.
Replication	All the clinical and immunological data was generated in laboratories within Shanghai Public Health Clinical Center which undertook regular quality controls and inter-laboratory consistency evaluations. All the genetic sequence data were generated using the standard practice of molecular biology and next generation sequencing standards.No experimental replication was performed for sequencing experiments and clinical measurements.
Randomization	Participants were chosen randomly.
Blinding	The measurements were performed without prior knowledge of the participant groups.

Reporting for specific materials, systems and methods

We require information from authors about some types of materials, experimental systems and methods used in many studies. Here, indicate whether each material, system or method listed is relevant to your study. If you are not sure if a list item applies to your research, read the appropriate section before selecting a response.

Materials & experimental systems

n/a	Involved in the study
☒	☐ Antibodies
☒	☐ Eukaryotic cell lines
☒	☐ Palaeontology
☒	☐ Animals and other organisms
☐	☒ Human research participants
☒	☐ Clinical data

Methods

n/a	Involved in the study
☒	☐ ChIP-seq
☒	☐ Flow cytometry
☒	☐ MRI-based neuroimaging

Human research participants

Policy information about studies involving human research participants

Population characteristics	A total of 326 patients, who were tested positive for SARS-CoV-2 RNA and were admitted into Shanghai Public Health Clinical Center from Jan 20th to Feb 25th. The median age of the patients was 51 years (range 15-88) with a male: female sex ratio of 1.10. 125 cases (38.34% had at least one co-morbidiy, the most common were hypertension (76 cases), diabetes (24 cases), coronary heart disease (13 cases), chronic hepatitis B (10 cases), chronic obstructive pulmonary disease (2 cases), chronic renal disease (2 cases) and cancer (3 cases).
Recruitment	All the available COVID-19 patients who were willing to participate in this study were recruited in this study. No self-selection biase existed to the best of our knowledge.
Ethics oversight	The study was approved by the ethics committee of the Shanghai Public Health Clinical Center (Approval No. YJ-2020-S015-01)

Note that full information on the approval of the study protocol must also be provided in the manuscript.